Research Journal of Applied Sciences, Engineering and Technology 13(7): 510-524, 2016
DOI:10.19026/rjaset.13.3011
ISSN: 2040-7459; e-ISSN: 2040-7467

Submitted: November 11, 2015 Accepted: February 10, 2016 Published: October 05, 2016

Research Article

Modeling CO_2-H_2S Corrosion of Tubular at Elevated Pressure and Temperature

Rida Elgaddafi, Ramadan Ahmed and Subhash Shah
University of Oklahoma, Sarkeys Energy Center, 100 Boyd St, Room 1180, Norman, OK 73019, USA

Abstract: This study is aimed at improving carbon steel corrosion prediction in CO_2-H_2S environment. Corrosion is one of the major challenges faced by the oil and gas industry. This is mainly because of corrosive nature of formation fluids. Often produced hydrocarbons are accompanied by brine containing acidic gases such as carbon dioxide and hydrogen sulfide. A number of CO_2-H_2S corrosion models have been developed to predict corrosion of carbon steel under low-pressure (partial pressures of CO_2 and H_2S less than 12 and 30 bar, respectively) and low-temperature. These models overestimate corrosion rate at high-pressure and high-temperature (HPHT) due to the application of the Henry's law in predicting solubility of CO_2 and H_2S in NaCl solution (brine) under HPHT. In this study, an improved corrosion model, which utilizes thermodynamic based gas solubility model, has been developed to predict concentration of corrosive gases (CO_2 and H_2S) in brine solution saturated with natural gas. The corrosion model is verified using experimental data available in the literature. Predominantly, model predictions show good agreement with corrosion rate measurements obtained under various conditions.

Keywords: Corrosion, tubular, carbon dioxide, hydrogen sulfide, pressure, temperature

INTRODUCTION

Corrosion process is complex and diverse. Different types of corrosion occur depending on conditions of corrosive environment. As a result, various mechanisms have been proposed to describe corrosion phenomena. In general, corrosion mechanisms are categorized as atomic, molecular, or ionic transport process that occurs at the interface of a metal and its surrounding environment. Corrosion process commonly involves more than one step and the slowest one controls process kinetics. Corrosion prevention is a major challenge in the industry. Corrosion related failures can lead to costly repair operations, plant shutdown, as well as health and environmental hazards. The presence of acidic gases such as CO_2 and H_2S in produced fluids increases corrosion in production and completion equipment. At present, CO_2 corrosion is becoming the most common issue because of CO_2-injection for enhanced oil recovery application and exploration of gas reservoirs containing acidic gases.

Corrosion mechanisms of carbon steel in aqueous CO_2-H_2S system have been studied by many researchers. Although corrosion of carbon steel in presence of H_2S or CO_2 has been investigated, understanding of the effect of H_2S on CO_2 corrosion is still limited. This is because the impact of H_2S on CO_2 corrosion is complicated. Generally, severity of CO_2-H_2S corrosion depends on pressure, temperature, pH, composition of the gas phase and partial pressures of CO_2 and H_2S.

Corrosion prediction is a key element in equipment design and well planning. A number of CO_2-H_2S corrosion models (Anderko and Young, 1999; Sun and Nesic, 2007; Nesic *et al*., 2008; Sun and Nešić, 2009; Nešić *et al*., 2009; Fardisi *et al*., 2012; Zheng *et al*., 2014) have been developed to forecast corrosion of carbon steel in presence of brine saturated with carbon dioxide and hydrogen sulfide. The models are often formulated based on types of corrosion scale, corrosion mechanism and rate-controlling phenomena involved in the corrosion process.

Under different operating conditions, various types of corrosion scale can be formed on steel surface in CO_2-H_2S environment. The type of corrosion scale mainly depends on H_2S partial pressure, temperature and solution pH. A mechanistic model for predicting uniform corrosion in aqueous CO_2-H_2S environment has been developed by Sun and Nešić (2009). The model is an extension of their earlier model (Sun and Nesic, 2007), which is formulated to predicted corrosion of carbon steel in pure H_2S system. Based on experimental observations, formation of two mackinawite layers on steel surface is considered in the modeling, assuming that H_2S effect dominates the

Corresponding Author: Ramadan Ahmed, University of Oklahoma, Sarkeys Energy Center, 100 Boyd St, Room 1180, Norman, OK 73019, USA, Tel.: (405) 325-0745; 405-325-7477

corrosion process. Therefore, it is expected that corrosion process is always under mass-transfer control rather than electrochemical or chemical kinetics control. Comparison of model predictions with available experimental data showed reasonable agreement at low CO_2 and H_2S partial pressure and relatively high temperature. However, the model does not account for iron sulfide precipitation and corrosion scale damage resulting from hydrodynamic effects.
The primary objectives of this investigation are:

- Better understanding for corrosion mechanism in presence of corrosion scale.
- Development of a theoretical model for predicting corrosion rate in aqueous CO_2-H_2S system at elevated pressure and temperature.
- Development of accurate solubility model that predicts concentrations of dissolved CO_2, H_2S and other species in brine solution at HPHT condition.
- Providing accurate prediction of solution pH in CO_2-H_2S environment.
- Validating accuracy of the new corrosion model and identifying effects of variables such as CO_2 and H_2S partial pressures, temperature and pH on carbon steel corrosion.

In this study, the model developed by Sun and Nešić (2009) is investigated and improved to describe uniform corrosion of carbon steel in aqueous CO_2-H_2S environment.

LITERATURE REVIEW

A number of investigations (Zhang *et al*., 2009; Choi and Nešić, 2011; Valdes *et al*., 1998; Smith and Pacheco, 2002; Srinivasan and Kane, 1996; Kvarekval *et al*., 2003; Mohammed Nor *et al*., 2014; Li *et al*., 2013, 2014; Schutt and Lyle, 1998; Fang *et al*., 2010; Yan *et al*., 2015) have been conducted on CO_2-H_2S corrosion of carbon steel studying effects of environmental conditions such as partial pressure of acidic gases, temperature, flow condition and water chemistry. Moreover, studies (Anderko, 2000; Sun *et al*., 2008; Kvarekval *et al*., 2003; Sun *et al*., 2006; Svenningsen *et al*., 2009) have been performed to examine the role of various corrosion products.

Different models have been developed to predict corrosion in aqueous CO_2-H_2S environment. A recent model (Anderko and Young, 1999) coupled the CO_2-H_2S corrosion model with a thermodynamic-based solubility model, which provides activities of species involved in corrosion process. The model predicts corrosion rate by analyzing electrochemical process that represents partial cathodic and anodic reactions occurring on steel surface. The electrochemical process include reduction of Hydrogen ions (H^+), carbonic acid (H_2CO_3), Hydrogen Sulfide (H_2S), water and oxidation of iron. The model accounts for formation of corrosion scale (iron carbonate and iron sulfide). For wide range of temperature (20 to 260°C) and solution pH (4 to 6), model predictions showed good agreement with experimental data obtained at 1 bar. Anderko and Young (1999) improved the original model to make predictions for CO_2 partial pressure of up to 30 bar, temperature of up to 200°C and H_2S concentration of up to 300 ppm.

Fluid velocity is one of the most relevant parameters affecting corrosion in presence of CO_2. Fluid flow facilitates corrosion due to enhancement of transport process of produced and consumed species in surrounding fluid and reduction of protective scale formation. High local fluid velocity at steel surface leads to more advanced type of corrosion by breaking protective scale and exposing the metal to corrosive fluid, resulting in localized corrosion.

Furthermore, during oil and gas production, flow through tubing can be a single or multiphase flow. Often multiphase flows are characterized by pressure and flow rate fluctuations, which affect formation of corrosion scale. Nesic *et al*. (2008) developed an improved model for predicting CO_2-H_2S corrosion in multiphase flows. The model combines a number of previously developed models (Nordsveen *et al*., 2003; Nešić *et al*., 2003; Nešic and Lee, 2003; Sun and Nesic, 2007; Nesic *et al*., 2008). Most of these models (Nordsveen *et al*., 2003; Nešić *et al*., 2003; Nešic and Lee, 2003) were developed to simulate corrosion process in pure CO_2 environment. Sun and Nesic (2007) formulated their model for corrosion occurring in pure H_2S system. Since the improved model (Nesic *et al*., 2008) incorporates all previous model features, it is applicable for a wide range of temperature (1 to 20°C), salinity (up to 25% wt NaCl) and H_2S partial pressure (0.001 mbar to 10 bar).

In the field, oil is often produced together with water, acidic gases (CO_2 and H_2S) and acetic acid (HAc). The mixture is highly corrosive and considered as main source of corrosion that can cause failure of production equipment and pipelines. According to recent experimental studies (Singer *et al*., 2007, 2010; Asmara and Ismail, 2011), presence of acetic acid accelerates aqueous CO_2-H_2S corrosion. Nešić *et al*. (2009) proposed a theoretical model to predict corrosion caused by aqueous CO_2, H_2S and organic acid assuming formation of iron carbonate and iron sulfide protective layers. CO_2 and organic acid corrosion is modeled considering electrochemical process; while H_2S corrosion is modeled based on mass transfer process occurring in mackinawite layer. The model features include:

- Describing corrosion mechanism
- Identifying major corrosive species
- Predicting H_2S concentration profile as a function of distance from steel surface.

Model predictions showed reasonable agreement with experimental data under wide range of test conditions.

Generally, corrosion process involves a series of steps that may affect its kinetics. The slowest step controls the overall corrosion process. In sour gas environment, CO_2/H_2S Partial Pressure Ratio (PPR) is considered as a key parameter in determining the effect of which gas dominates the corrosion process (Smith and Pacheco, 2002; Woollam *et al*., 2011). A recent mechanistic model for predicting uniform corrosion in sour environment is developed by Fardisi *et al*. (2012). The model incorporates transient chemical reactions, transport of active species to and away from exposed steel surface and electrochemical reactions at the surface. The model simulates impact of corrosion scale considering formation of iron sulfide and neglecting formation of iron carbonate scale. In other words, it assumes CO_2 facilitates corrosion by promoting electrochemical reaction; while H_2S controls scale formation. These assumptions are valid when P_{CO2}/P_{H2S} is less than 500. Model predictions show reasonable agreement with experimental measurements.

The most recent electrochemical model (Zheng *et al*., 2014) has been formulated to predict effect of H_2S on CO_2 corrosion for short-term exposure prior to formation of iron sulfide scale. The model is based on electrochemical reaction that occurs due to reactions of carbonate species, sulfide species and hydrogen ions at steel surface. Model predictions show good agreement with experimental data for short-term exposure; however, it overestimates corrosion rate when applied for long-term exposure. The discrepancy is attributed to the formation of iron sulfide scale, which is not considered in the model formulation.

MATERIAL AND METHODS

Solubility of acidic gases has a strong impact on corrosion process. A model developed in this study combines CO_2-H_2S corrosion model with improved thermodynamic-based solubility model. It also accounts for presence of protective layer.

Gas solubility model: The improved solubility model for acidic gases has been developed based on existing models (Duan *et al*., 2007; Duan and Sun, 2003; Mao and Duan, 2006; Duan and Mao, 2006; Zirrahi *et al*., 2012). The model is specially formulated to predict solubility of common acidic gases in brine under HPHT condition. The amount of CO_2 and H_2S dissolved in brine is utilized to calculate the concentration of hydrogen ions resulting from dissolution of these gases under equilibrium condition. Existing dissociation equations (Millero, 1986; Hershey *et al*., 1988; Millero *et al*., 2007; Sun *et al*., 2008) are used to predict bulk concentration of hydrogen ions. The bulk concentration of H^+ along with concentrations of CO_2 and H_2S are used to determine corrosion rate caused by each species as presented in CO_2-H_2S Corrosion model.

Theoretical solubility models, applicable for aqueous solutions, are based on maintaining chemical potential balanced between gas and liquid phases. Since unknown amount of water vapor exists in the gas phase under equilibrium condition, an iterative numerical procedure is needed to determine composition of the gas phase. In this study, to avoid the numerical procedure, semi-empirical equation developed by Duan and Mao (2006) is utilized to estimate mole fraction of water vapor as:

$$y_{H_2O} = \frac{x_{H_2O}.P^S_{H_2O}}{\varphi_{H_2O}.P}\exp\left(\frac{\upsilon'_{H_2O}.\left(P - P^S_{H_2O}\right)}{RT}\right) \quad (1)$$

where, x_{H_2O} is mole fraction of water in liquid phase, which is approximately 1 for CO_2-H_2S system. $P^S_{H_2O}$ and υ'_{H_2O} are water saturation pressure and molar volume of liquid, respectively. φ_{H_2S} is fugacity coefficient of water in gas phase, which is obtained from an empirical model presented in Appendix A. After mole fraction of water vapor is obtained, mole fractions of other gas components are updated applying the material balance equation and then new gas phase mole fractions are utilized in the solubility calculation.

Under equilibrium condition, a number of homogenous chemical reactions occur in aqueous CO_2-H_2S system including CO_2 and H_2S dissolution in brine, which are described as follows:

$$CO_{2(g)} \rightarrow CO_{2(aq)} \quad (2)$$

$$H_2S_{(g)} \longrightarrow H_2S_{(aq)} \quad (3)$$

Dissolved amount of CO_2 and H_2S can be computed using more advanced and accurate CO_2 and H_2S solubility model (Duan *et al*., 2007; Duan and Sun, 2003). Molality of CO_2 and H_2S in the bulk solution is given by:

$$\ln m_i = \ln\left(y_i \times \varphi_i \times P\right) - \frac{\mu_i^{l(0)}}{RT} - \ln \gamma_i \quad (4)$$

Subscript i denotes acidic components of the gas phase (CO_2 and H_2S); y_i is the new mole fraction of component i in the gas phase after normalization; φ_i is the fugacity coefficient for component i in the gas phase, which are calculated based on the Peng-Robinson equation of state; P is total pressure. In Eq. (4), $\mu_i^{l(0)} / RT$ term is called interaction parameter, Par (T, P). The parameter is a function of temperature and pressure. It is predicted using empirical model and interaction parameter coefficients (T-P coefficients), which are presented in Appendix A. Activity coefficients of various gas species in Eq. (4), ln γ_i, are determined as (Duan *et al*., 2007; Duan and Sun, 2003):

$$\ln \gamma_i = \sum_c 2\lambda_{i-c} m_c + \sum_a 2\lambda_{i-a} m_a + \sum_c \sum_a \zeta_{i-c-a} m_c m_a \quad (5)$$

where, subscript of m_c and m_a denotes anions and cations molality, respectively, λ_{i-a} and, ζ_{i-c-a} are the second and third order interaction parameters, respectively. The parameters are calculated with appropriate T-P coefficients. Subscripts *a* and *c* denote anion and cation, respectively.

In aqueous liquids, considerable amount of dissolved CO_2 hydrates and creates carbonic acid:

$$CO_{2(aq)} + H_2O \xleftrightarrow{K_{hyd}} H_2CO_3 \quad (6)$$

$$K_{hyd} = \frac{C_{H_2CO_3}}{CO_2} \quad (7)$$

In addition, carbonic acid and hydrogen sulfide dissociate and produce several ions according to the following Eq. (8) to (15):

$$H_2CO_3 \xleftrightarrow{K_{CO_2,1}} H^+ + HCO_3^- \quad (8)$$

$$K_{CO_2,1} = \frac{C_{HCO_3^-} \times C_{H^+}}{C_{H_2CO_3}} \quad (9)$$

$$HCO_3^- \xleftrightarrow{K_{CO_2,2}} H^+ + CO_3^- \quad (10)$$

$$K_{CO_2,2} = \frac{C_{CO_3^-} \times C_{H^+}}{C_{HCO_3^-}} \quad (11)$$

$$H_2S_{(aq)} \xrightarrow{K_{H_2S,1}} H^+ + HS^- \quad (12)$$

$$K_{H_2S,1} = \frac{C_{H^+} \times C_{HS^-}}{C_{H_2S(aq)}} \quad (13)$$

$$H_2O \xrightarrow{K_W} H^+ + OH^- \quad (14)$$

$$K_w = \frac{C_{H^+} \times C_{OH^-}}{C_{H_2O}} \quad (15)$$

where, $C_{H_2CO_3}$ is concentration of carbonic acid.

$C_{HCO_3^-}$, $C_{CO_3^{2-}}$, C_{H^+}, C_{HS^-} and C_{OH^-} are concentrations of bicarbonate, carbonate, hydrogen, bisulfide and hydroxide ions, respectively. K_{hyd}, $K_{CO_2,1}$, $K_{CO_2,2}$, $K_{H_2S_1}$ are chemical equilibrium constants of reactions occurring in the liquid phase. The constants are functions of temperature and brine concentration as presented in Appendix A. There are six unknowns ($C_{H_2CO_3}$, $C_{HCO_3^-}$, $C_{CO_3^{2-}}$, C_{H^+}, C_{HS^-}, C_{OH^-}) in the model Eq. (8) to (17). In aqueous CO_2-H_2S system, electro-neutrality can be described using the following formula:

$$C_{H^+} = C_{OH^-} + C_{HCO_3^-} + 2C_{CO_3^{2-}} + C_{HS^-} \quad (16)$$

Carbon in the system is preserved during corrosion process. Hence, carbon material balance of the system can be expressed as:

$$C_{CO_2} = C_{H_2CO_3} + C_{HCO_3^-} + C_{CO_3^{2-}} \quad (17)$$

Model equations form a system of non-linear equations, which requires numerical procedure to predict corrosion. To solve the system of equations numerically, a computer program is developed using Mathlab. The program predicts bulk concentration of

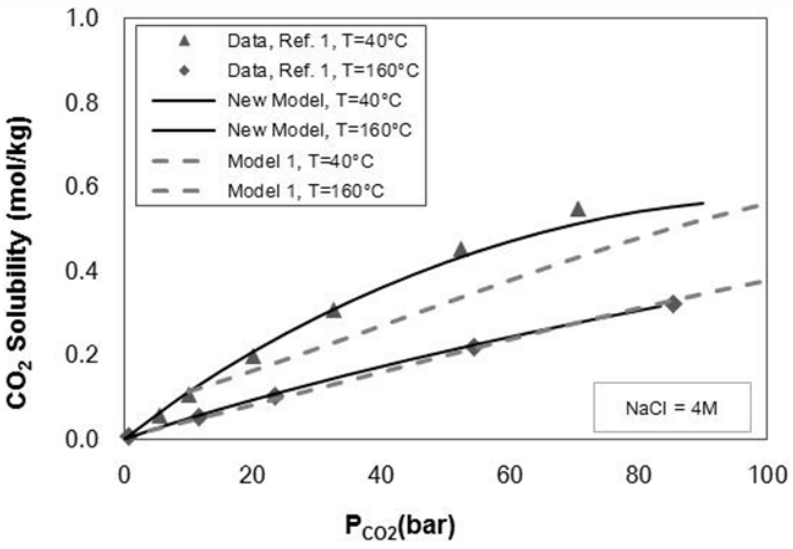

Fig. 1: Comparison of model prediction with experimental data at various temperatures

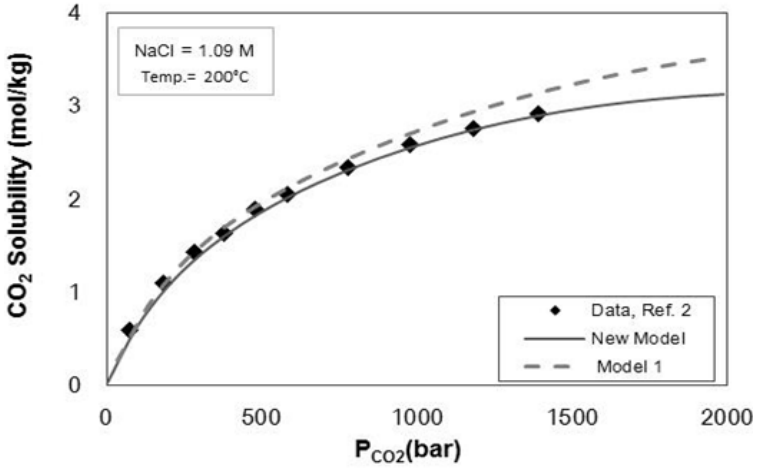

Fig. 2: Comparison of present model with existing model

Table 1: Experimental data from previous studies

No.	Reference	Case	CR(mm/y)
1	Rumpf *et al*. (1994)		-
2	Takenouchi and Kennedy (1965)		-
3	Mohamed *et al*. (2011)		-
4	Meyssami *et al*. (1992)		-
5	Kvarekval *et al*. (2003)	A	2.00
		B	1.90
		C	0.86
		D	0.80
		E	2.10
		F	0.71
6	Bich and Goerz (1996)	A	0.77
		B	0.47
		C	0.98
		D	0.99
		E	1.32
7	Kvarekval *et al*. (2005)	A	0.84
		B	0.53
		C	1.20
8	Li *et al*. (2012)		0.50
			0.28
			0.37
			1.25
			0.48
			0.19
			0.28
			0.92
9	Zhang *et al*. (2009)		0.20
			0.35
			0.81
			2.18
10	Zhang *et al*. (2011)		0.23
			0.59
			0.92
			1.73
			1.43
			1.54
			2.00
			2.30
			1.69
			1.28

species in aqueous solution as a function of temperature and pressure. Solution pH is traditionally defined as: $pH = -\log \left[C_{H^+}\right]$. Hydrogen ion concentration is determined from Eq. (16). To validate accuracy of the solubility model, predictions are compared (Fig. 1 and 2) with published measurements (Table 1) and predictions of existing model (Model 1). A complete list of existing models used in the evaluation of the new models is presented in Table 2. At 40°C, the new solubility model has better accuracy than existing model.

Table 2: Existing models used to validate new models

Name	Reference	Model type
Model 1	Duan and Sun (2003)	Solubility
Model 2	Mohamed *et al*. (2011)	Solubility
Model 3	Choi and Nešić (2011)	Corrosion
Model 4	Sun and Nešić (2009)	Corrosion
Model 5	Fardisi *et al*. (2012)	Corrosion

Effect of CO_2 partial pressure and temperature on solution pH is shown in Fig. 3. New and existing (Meyssami *et al*., 1992; Mohamed *et al*., 2011; Choi and Nešić, 2011) model predictions and measurements show similar trend and good agreement in most cases. The pH gradually decreased with increase in CO_2 partial pressure and temperature. This change is related to effects of pressure and temperature on CO_2 solubility in brine (i.e. concentrations of carbonic species increase with CO_2 partial pressure whereas their concentrations decrease with temperature).

CO_2-H_2S corrosion model: Accurate prediction of corrosion rate in HPHT sour environment is critical for oilfield applications. As described earlier, various corrosion models are available for aqueous CO_2 and CO_2-H_2S systems. In this study, an existing model (Sun and Nešić, 2009) is improved to predict corrosion in aqueous H_2S and CO_2-H_2S environment under HPHT condition. The improvement includes:

- Predicting bulk concentration of active species using accurate solubility model as presented in Gas Solubility Model.

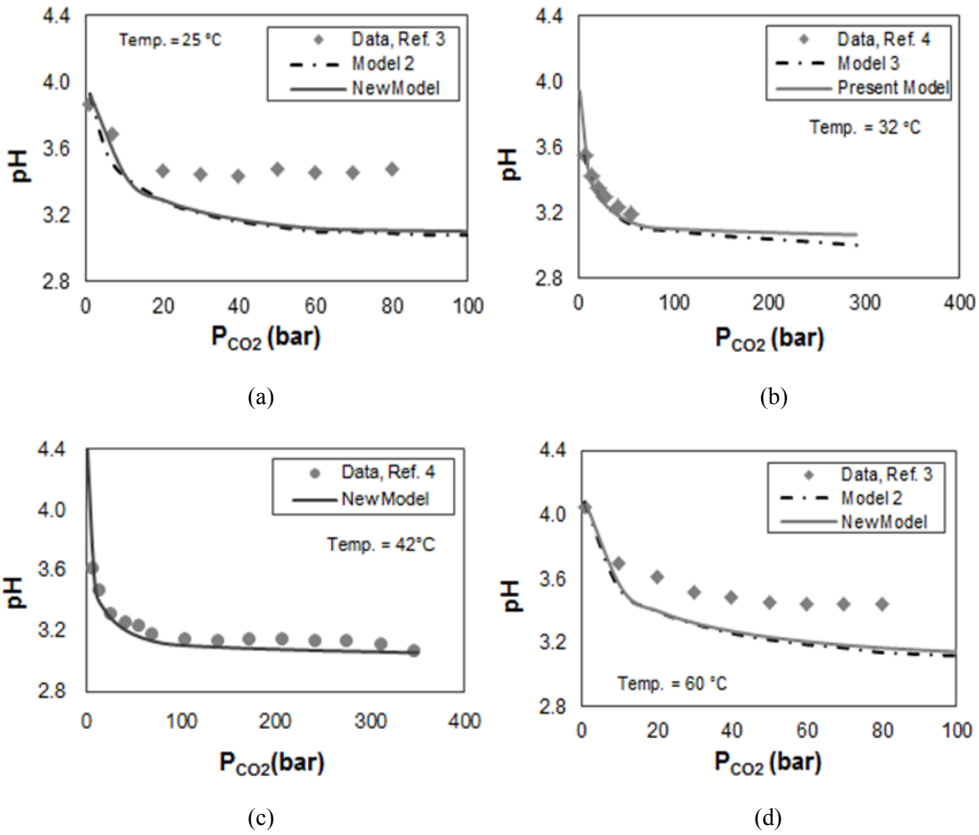

Fig. 3: Comparison between pH measurements and modeling results at a) 25°C, b) 32°C, c) 42°C and d) 60°C

- Modifying diffusion and mass transfer coefficients to account for effects of temperature and fluid velocity. The model takes into account effects of H_2S concentration, temperature, fluid velocity and protectiveness of corrosion scale (mackinawite layer) on corrosion process. Thickness and type of mackinawite layer formed on steel surface change with time and depend on scale formation and removal rates. According to observations of Sun and Nesic (2007), mackinawite layer is predominantly iron sulfide, which is formed due to direct reaction of H_2S with metal surface (Fig. 4). Based on experimental results and theoretical analysis, the following assumptions are often made in developing a mathematical model for aqueous CO_2-H_2S corrosion of steel:
- Corrosion in aqueous H_2S system occurs via direct heterogeneous solid-state reaction at steel surface and the overall reaction can be expressed as:

$$Fe_{(S)} + H_2S \rightarrow FeS_{(S)} + H_2 \quad (18)$$

- Immediately after exposure, very thin and dense mackinawite film (less than 1 μm) forms on steel surface.
- The thin mackinawite layer continuously goes through a cyclic process that includes scale growth, cracking and delamination, which creates the outer mackinawite layer.
- A thicker (greater than 1 μm) and loosely porous outer mackinawite layer is formed on top of the thin layer.

In order to develop a generalized model, effects of H_2S, pH, CO_2 and protective scale on corrosion are modeled separately.

Effect of H_2S: Corrosion of steel in aqueous CO_2-H_2S environment involves chemical reactions, mass transport and charge transfer processes. Due to formation of mackinawite layers (inner and outer), it is assumed that the corrosion is always under mass transfer control rather than electrochemical or chemical reaction control. A schematic shown in Fig. 4 demonstrates corrosion related processes occurring in aqueous solutions saturated with CO_2 and H_2S gases.

During corrosion process (Fig. 4), reactive ions are transported by diffusion caused by concentration gradients. Different types of diffusion processes are involved including: convective diffusion in surrounding fluid, molecular diffusion through porous outer layer and solid-state diffusion through thin mackinawite layer. Thus, molecular/ionic fluxes (mol/m^2.s) of the three diffusion process can be written as:

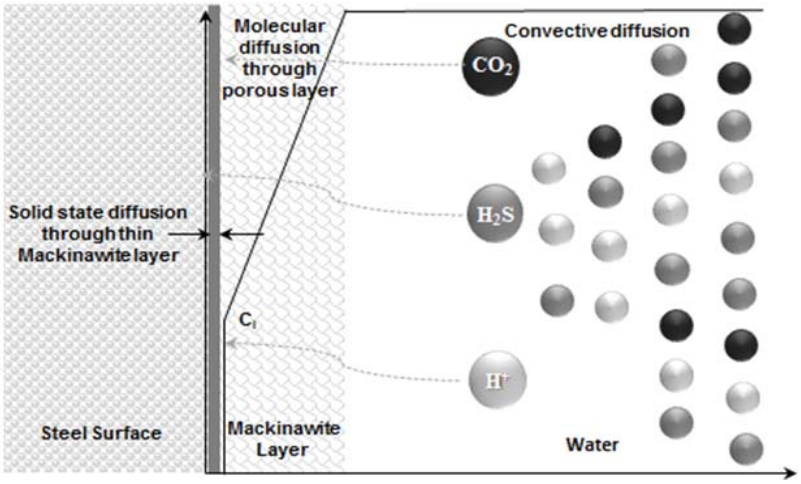

Fig. 4: Schematic of H_2S corrosion process (adopted from Sun and Nešić, 2009)

- Convective diffusion through the surrounding fluid as:

$$Flux_Z = K_{mZ}.(C_{b,Z} - C_{o,Z}) \quad (19)$$

- Molecular diffusion through outer layer:

$$Flux_Z = \frac{D_Z \varepsilon \psi}{\delta_{OS}}(C_{o,Z} - C_{i,Z}) \quad (20)$$

- Solid-state diffusion through inner mackinawite film:

$$Flux_Z = A_Z \ln\left(\frac{C_{i,Z}}{C_{s,Z}}\right) \quad (21)$$

where, subscript Z denotes components. H_2S, H^+, CO_2 and C_b, are concentrations of different species in bulk solution. C_o, C_i and C_s represent concentrations of different species at outer scale-solution interface, inner scale-film interface and steel surface, respectively. Under steady state condition, the three fluxes for each single component are equal to each other and are related to the corrosion rate as: $CR_Z = Flux_Z.M_{Fe}/\rho_{Fe}$, where M_{Fe} and ρ_{Fe} are molecular weight and density of iron, respectively. By eliminating unknown interfacial concentrations from Eq. (19) through (21), the flux of H_2S can be described as:

$$Flux_{H_2S} = A_{H_2S} \ln \frac{C_{b,H_2S} - Flux_{H_2S}\left(\frac{\delta_{0.5}}{D_{H_2S}\varepsilon\psi} + \frac{1}{K_{m,H_2S}}\right)}{C_{s,H_2S}} \quad (22)$$

Effect of pH: Surrounding environment pH has a significant impact on corrosion. Although mackinawite layers form and control corrosion process due to direct reaction of dissolved H_2S with steel surface, the process is strongly driven by reduction of protons rather than the direct reaction. Proton transport rate (flux of proton) is controlled by convective diffusion, diffusion through the pores outer layer and solid-state diffusion through thin mackinawite layer. Fluxes of protons through the three layers are obtained from Eq. (19-21). At steady state condition, the three fluxes of H^+ are equal and relate to the corrosion rate as: $CR_{H^+} = Flux_{H^+}.M_{Fe}/2\rho_{Fe}$. The flux of protons, which is controlled by mackinawite layer, is expressed as:

$$Flux_{H^+} = A_{H^+} \ln \frac{C_{b,H^+} - Flux_{H^+}\left(\frac{\delta_{0.5}}{D_{H^+}\varepsilon\psi} + \frac{1}{K_{m,H^+}}\right)}{C_{s,H^+}} \quad (23)$$

Effect of CO_2: In aqueous CO_2-H_2S system, mass transfer predominantly controls corrosion process. Hence, the flux of CO_2 can be obtained by applying the methods used in determining H_2S and H^+ effects on corrosion. Accordingly, at steady state condition, the three fluxes of CO_2 must be equal and relate to CO_2 corrosion rate as: $CR_{CO_2} = Flux_{CO_2}.M_{Fe}/\rho_{Fe}$. Hence, the flux of CO_2 is given by:

$$Flux_{CO_2} = A_{CO_2} \ln \frac{C_{b,CO_2} - Flux_{CO_2}\left(\frac{\delta_{0.5}}{D_{CO_2}\varepsilon\psi} + \frac{1}{K_{m,CO_2}}\right)}{C_{s,CO_2}} \quad (24)$$

Hydration of CO_2 produces corrosive species (H_2CO_3), which need to be included in corrosion modeling. The hydration has the potential to strongly affect corrosion. Therefore, CO_2 flux can be equated to the limiting rate of hydration at steel surface as:

Table 3: Experimental conditions (Kvarekval *et al*., 2003)

			Gas Composition	
Case No.	Time (h)	T(°C)	P_{CO2} (bar)	P_{H2S} (bar)
A	24	120	6.90	1.38
B	20	120	6.90	2.76
C	138	120	6.90	2.76
D	166	120	6.90	2.76
E	21.5	120	6.90	3.45
F	383	120	6.90	3.45
G	68.5	120	6.90	4.14

$$\text{Flux}_{CO_2} = C_{s,CO_2}\left(D_{H_2CO_3}.\varepsilon.\psi.K_{hyd}^{f}.K_{hyd}\right)^{0.5} \quad (25)$$

By eliminating the unknown variable, C_{s,CO_2} from Eqns. (24) and (25), CO_2 flux can be expressed as:

$$\text{Flux}_{CO_2} = A_{CO_2}\ln\frac{C_{b,CO_2} - \text{Flux}_{CO_2}\left(\frac{\delta_{0.5}}{D_{CO_2}\varepsilon\psi} + \frac{1}{K_{m,CO_2}}\right)}{\frac{\text{Flux}_{CO_2}}{\left(D_{H_2CO_3}.\varepsilon\varepsilon\psi\,{}_{hyd}^{f}.K_{hyd}\right)^{0.5}}} \quad (26)$$

The bulk concentration of carbon dioxide, $C_{b,CO2,}$ at a given pressure and temperature can be obtained using Eq. (4). The total corrosion rate in aqueous CO_2-H_2S system is equal to the sum of rates of corrosion caused by H_2S, H^+ and CO_2. Hence:

$$CR_T = CR_{H_2S} + CR_{H^+} + CR_{CO_2} \quad (27)$$

Effect of corrosion scale: Due to continuous precipitation of corrosion products, thickness of outer sulfide layer changes with time. It is assumed that thickness of the layer depends on difference between layer-formation and layer-damage rates, which can be expressed as:

$$SRR = SFR - SDR \quad (28)$$

where, SRR, SFR and SDR are sulfide retention rate, sulfide layer-formation rate and sulfide layer-damage rate, which all are in units of (mol/m^2.s). For typical application range (i.e., pH between 4 and 5), precipitation and dissolution of iron sulfide layer have no significant role; therefore, Eq. (28) can be written as:

$$SRR = CR - SDR_m \quad (29)$$

where, SDRm is measured sulfide layer mechanical damage rate, which is estimated as (Sun *et al*., 2008): $SDR_m \approx 0.5CR$. When the layer retention rate is obtained, change in mass of the outer sulfide layer can be calculated as:

$$\Delta m_{os} = SRR \times M_{FeS} \times A \times \Delta t \quad (30)$$

where,
M_{FeS} : Molecular weight of iron sulfide in kg/mol
Δt : The time interval in seconds

In Eq. (26), mackinawite layer porosity and tortuosity factor are needed to compute flux of CO_2. Porosity of outer mackinawite layer is expected to be very high ($\varepsilon \approx 0.9$) and tortuosity factor (ψ) is estimated to be 0.003. Then, thickness of mackinawite layer is given by:

$$\delta_{os} = \Delta m_{os}/(\rho_{FeS} \times A) \quad (31)$$

Equations (22, 23 and 26) are nonlinear with respect to variable Flux_Z, which cannot be expressed explicitly. Therefore, solutions for these equations are obtained numerically using the Newton-Raphson method. More details of the numerical procedure are presented elsewhere (Sun and Nešić, 2009).

RESULTS AND DISCUSSION

Model evaluation: The CO_2-H_2S corrosion model is enhanced by introducing new correlations for thermodynamic properties of corrosive gases. In addition to the corrosion rate, the model predicts CO_2 and H_2S concentrations and other corrosive species in brine and pH under moderate pressure and temperature. To assess accuracy of the new model, its predictions are validated using available experimental data. To assess impact of hydrogen sulfide partial pressure on corrosion rate, model predictions are compared with experimental data obtained under different operating conditions (Table 3). The experiments were conducted at HPHT condition varying exposure time from 20 to 383 h.

As depicted in Fig. 5, the new model in most cases provides reasonable predictions. In some cases (Case F), moderate discrepancies are observed. In most cases, the model slightly under-predicts corrosion rate. The comparison generally shows acceptable agreement between model predictions and experimental data.

In Fig. 6, predictions of the new and original models (Sun and Nešić, 2009) are compared with experimental data (Kvarekval *et al*., 2005). The measurements were obtained at relatively high

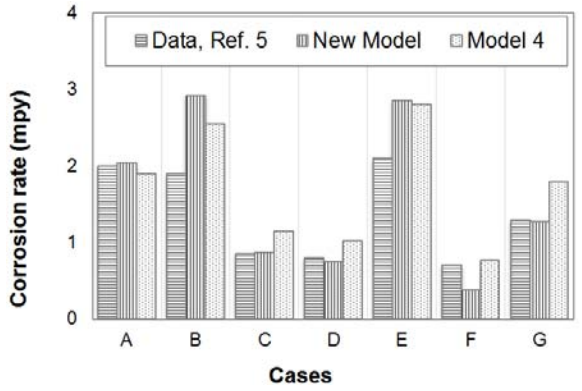

Fig. 5: Comparison of model predictions with experimental measurements (Kvarekval *et al*., 2003)

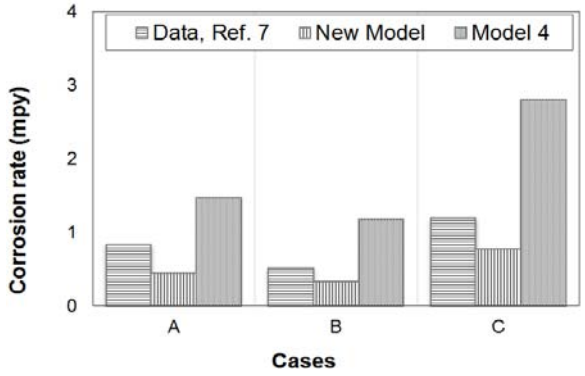

Fig. 6: Comparison of model predictions with measurements (Kvarekval *et al*., 2005)

Table 4: Experimental conditions (Omer *et al*., 2005)

			Gas composition	
Case No.	Time (h)	T (°C)	P_{CO2} (bar)	P_{H2S} (bar)
A	456	80	3.30	10.00
B	504	25	3.30	10.00
C	360	80	10.00	30.00

temperature and high H_2S concentration (Table 4). The proposed model exhibits better accuracy than original model, which overestimates corrosion rate due to inaccuracy of the Henry's law at high pressures (Fig. 7). Similar results were reported when H_2S solubility model predictions were compared with experimental measurements (Kumar *et al*., 2014)

To ensure applicability of the new model for wide range of pressure and temperature, model predictions are further validated with experimental data (Bich and Goerz, 1996) obtained at high temperature (120°C) and various CO_2-H_2S partial pressure ratios (Table 5). In addition, the model is compared (Fig. 8) with a previous mechanistic model (Fardisi *et al*., 2012). In most cases, the present model shows better accuracy than the previous model.

Figure 9 compares model predictions with measurement obtained from previous studies (Zhang *et al*., 2009, 2011; Jingen *et al*., 2011; Yin *et al*., 2008; Li *et al*., 2012) under different test conditions. Overall, the model provides reasonable predictions. Some data points display considerable scattering resulting from very sensitive nature of corrosion to the formation of protective scale.

In this study, accuracy of the existing model (Sun and Nešić, 2009) is improved and its applicability is extended to high pressure (CO_2 and H_2S partial pressure of 30 bar) and elevated temperature. Accuracy of the model diminishes beyond its application range Pitting corrosion, which is not considered in the current model formulation can occur when partial pressure is more than 30 bar.

Sensitivity analysis: In previous section, new model predictions are validated. It is well known that corrosion rate trend is affected by surrounding conditions such as:

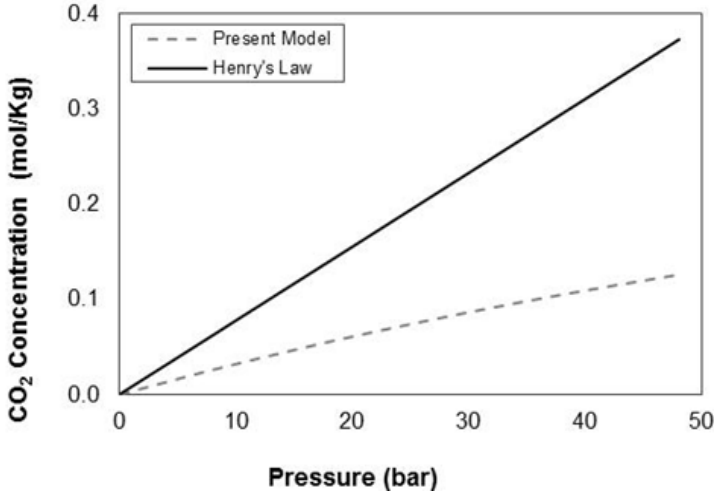

Fig. 7: Comparison of CO_2 concentration obtained from Henry's law and present model

Table 5: Experimental conditions (Bich and Goerz, 1996)

			Gas composition	
Case No.	Time (h)	T (°C)	P_{CO2} (bar)	P_{H2S} (bar)
A	71	60	5.3	3.0
B	91	60	5.3	3.0
C	69	65	3.5	12.2
D	91	65	12.8	8.0
E	63	65	3.0	4.2

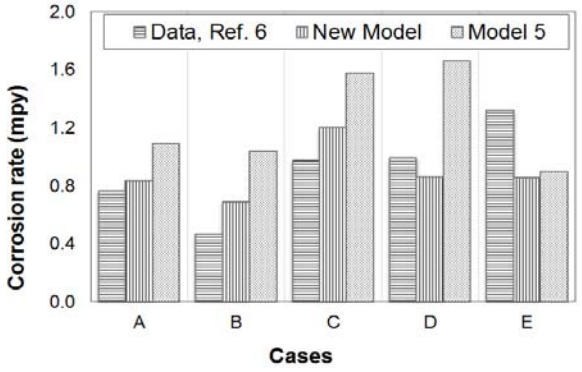

Fig. 8: Comparison of model predictions with experimental measurements (Bich and Goerz, 1996)

- H_2S and CO_2 partial pressures.
- Solution pH.
- Temperature.

To further assess model performance in terms of trend prediction, sensitivity analysis is performed by varying pH, H_2S partial pressure and temperature. Figure 10 shows predicted corrosion rate as a function of pH at 25°C. The model prediction simulates 72 h of exposure. As depicted from the plot, corrosion rate continuously decreases with increase in solution pH. A change in pH of the surrounding fluid system from 4 to 6 has negligible impact on corrosion rate. Corrosion rate trend with pH is in agreement with findings of a previous experimental study (Brown *et al*., 2004).

The influence of pressure on CO_2 corrosion is not fully understood. Increasing pressure at constant PPR increases partial pressure of H_2S. Presence of H_2S can either accelerate or slowdown corrosion process, depending on environmental condition (Schmitt, 1991; Videm and Kvarekvål, 1995; Ikeda *et al*., 1985). H_2S accelerates corrosion by acting as a promotor of anodic

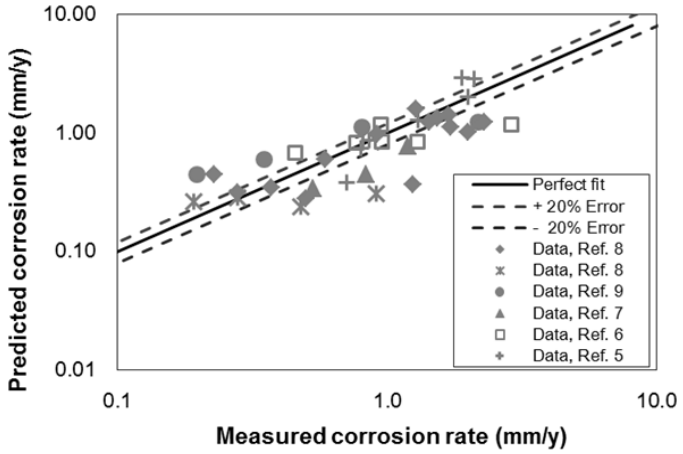

Fig. 9: Predicted vs. measured corrosion rate under wide range of test conditions

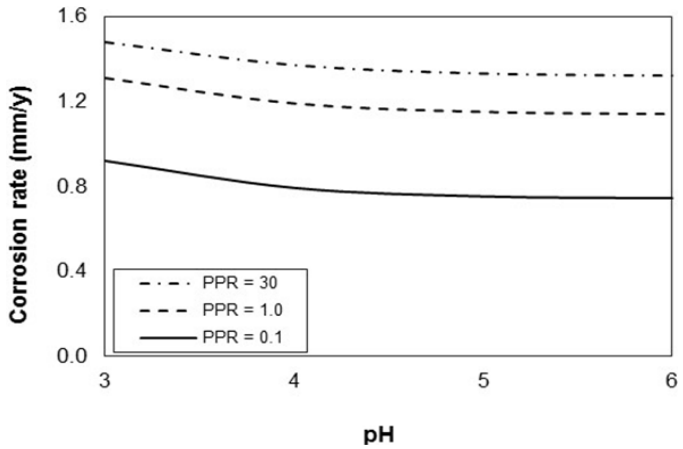

Fig. 10: Predicted corrosion rate vs. solution pH at P_{H2S} = 20 bar, P_{CO2} = 10 bar and Temp. = 25°C, t = 72 hr

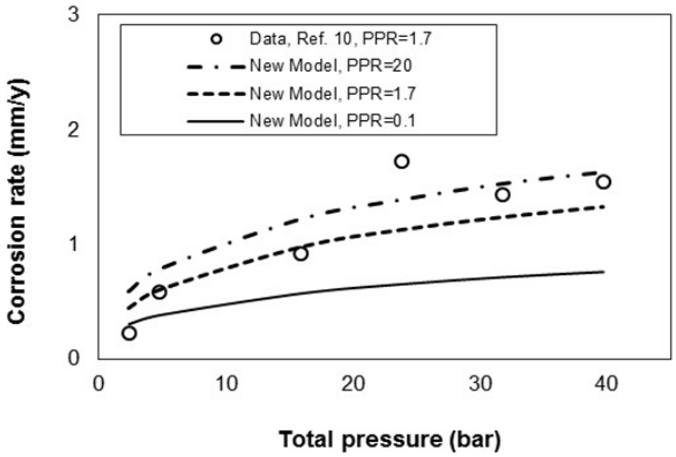

Fig. 11: Average corrosion rate vs. total pressure at P_{H2S}/P_{CO2} = 1.7 and Temp. = 60°C, t=120 hr

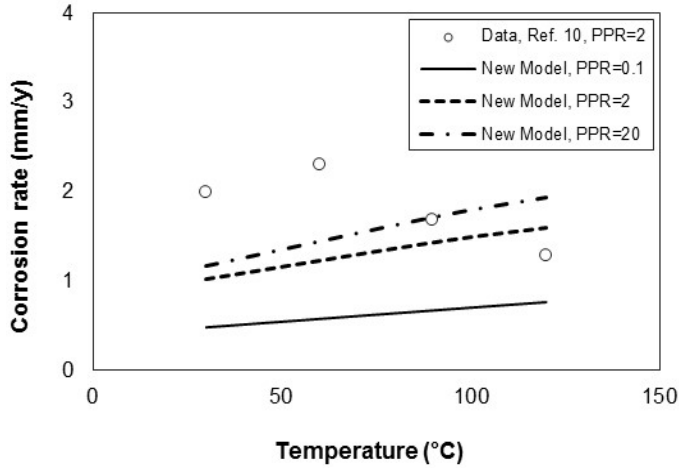

Fig. 12: Average corrosion rate vs. temperature at P_{H2S} = 12 bar, P_{CO2} = 6 bar and t = 96 hr

dissolution through the sulfide adsorption and affecting pH. On the other hand, H_2S can reduce corrosion by forming a protective layer on steel surface due to direct chemical reaction. Figure 11 compares model predictions with measurements (Zhang *et al*., 2009). Corrosion rate increased with pressure. Except for one outlier (p = 24 bar), the model predictions show satisfactory agreement with measurements.

Figure 12 shows influence of temperature on corrosion rate. Experimental measurements reported by Zhang *et al*. (2011) are used for comparison. The present model correctly predicts corrosion rate trend at low temperatures (less than 60°C), in which the corrosion rate increases with temperature. However, considerable discrepancy between the measurements and predictions is observed due to occurrence of pitting at low temperature. At high temperatures (more than 60°C), corrosion scale became more dense and compact due to structural transformation from mackinawite to other crystalline forms. This results in declining of corrosion rate with temperature. The current model does not account for the scale transformation.

CONCLUSION

Solubility of corrosives gases (CO_2 and H_2S) in brine solution was investigated theoretically considering wide range of pressure, temperature and ionic strength. A solubility model is developed and incorporated into CO_2-H_2S corrosion model to improve its performance. Model accuracy is extensively evaluated using published corrosion data. Based on this work, the following conclusions can be drawn:

- The improved CO_2-H_2S corrosion model shows reasonable accuracy when compared with experiment data obtained under wide range of environmental conditions.
- The model has reasonably responded to the environmental variations and indicated that temperature and partial pressure of CO_2 and H_2S are the most influential parameters.
- Formation of corrosion scales in CO_2-H_2S environment is deemed as the major factor influencing corrosion behavior of carbon steels.

Table 6: Constants for interaction parameters

T-P Coefficient	μ/T	$\lambda_{CO2\text{-}Na}$	$\xi_{CO2\text{-}Na\text{-}Cl}$
C_1	2.89E+01	-4.11E-01	3.36E-03
C_2	-3.55E-02	6.08E-04	-1.98E-05
C_3	-4.77E+03	9.75E+01	
C_4	1.03E-05		
C_5	3.38E+01		
C_6	9.04E-03		
C_7	-1.15E-03		
C_8	-3.07E-01	-2.38E-02	2.12E-03
C_9	-9.07E-02	1.71E-02	-5.25E-03
C_{10}	9.33E-04		
C_{11}		1.41E-05	

Table 7: Constants for interaction parameters

T-P Coefficient	μ/T	$\lambda_{H2S\text{-}Na}$	$\xi_{H2S\text{-}Na\text{-}Cl}$
C1	42.564	8.50E-02	-1.08E-02
C2	-0.0862	3.53E-05	
C3	-6084.37	-1.588261	
C4	6.87E-05		
C5	-102.768		
C6	8.45E-04	1.189E-05	
C7	-1.05907		
C8	3.57E-03		

Table 8: Constants for interaction parameters

T-P Coefficient	μCH4/T	$\lambda_{CH4\text{-}Na}$	$\xi_{CH4\text{-}Na\text{-}Cl}$
C1	8.31E+00	-8.12E-01	-2.99E-03
C2	-7.28E-04	1.06E-03	
C3	2.15E+03	1.89E+02	
C4	-1.40E-05		
C5	-6.67E+05		
C6	7.70E-03	4.41E-05	
C7	-5.03E-06		
C8	-3.01E+00		
C9	4.84E+02		
C10	8.31E+00	-4.68E-11	

Table 9: Constants of the water fugacity coefficient

Parameters	Value
a_1	-0.142006707
a_2	1.08369910*10E-02
a_3	-1.59213E-05
a_4	-0.000110805
a_5	-31.4287155
a_6	1.06338095*10E-03

- Protective properties of corrosion scales depend on the environmental conditions (temperature, CO_2 and H_2S partial pressures and pH) and the characteristics of the material.
- There is a general consensus on the influence of H_2S on CO_2 corrosion of carbon steel that, the presence of small concentration of H_2S (less than 10 ppm) in CO_2 saturated fluid tends to facilitate the corrosion rate while at higher concentration (more than 10 ppm), the corrosion rate decreases due to the formation of iron sulfide protective scale.

ACKNOWLEDGMENT

The authors would like to thank the Bureau of Safety and Environmental Enforcement (BSEE) for sponsoring this project (E12PC00035) and University of Oklahoma for providing the necessary support. Technical contributions from the industry advisory board members are also appreciated.

APPENDIX A

CO_2 solubility parameters: The interaction parameters involved in CO_2 solubility calculation can be estimated from the following generalized equation as:

$$\begin{aligned}\mathrm{Par}(T,P) &= C_1 + C_2T + C_3/T + C_4T^2 + C_5/(630-T) + C_6P \\ &+ C_7P\ln T + C_8P/T + C_9P/(630-T) + C_{10}P^2/(630-T)^2 \\ &+ C_{11}T\ln P\end{aligned} \quad (32)$$

where, C_1 to C_{11} are the T-P coefficients, which are given in Table 6.

The first and second dissociation constants of carbon dioxide in the pK form (i.e., pk_i = -log (K_i)) are estimated using correlation presented by Millero *et al*. (2007). The model is valid for temperature up to 482°F and NaCl concentration up to 6 M:

$$pK^*_{CO2,i} - pK_{CO_2,i} = A_i + B_i/T + C_i \times \ln T \quad (33)$$

where, pK_i is a dissociation constant corresponding to pure water and parameters Ai, Bi, Ci are function of molality. T is absolute temperature in Kelvin and subscript i refers to 1 and 2 to represent first and second dissociation, respectively:

$$\begin{aligned}pK_{CO_{2,1}} &= -402.56788 + 11656.46/T + 72.173\ln T - 0.161325T \\ &+ 7.5526\times10^{-5}T^2\end{aligned} \quad (34)$$

$$pK_{CO_2,2} = -122.49 + 5811.18/T + 20.52\ln T - 0.01209T \quad (35)$$

Parameters in Eq. (33), A_1, A_2, B_1, B_2, C_1, C_2, can be calculated using the following correlations:

$$A_1 = 31.3616m^{0.5} + 0.86644m - 0.33611m^{1.5} + 0.05888m^2$$
$$B_1 = -1422.25317\,m^{0.5}$$
$$C_1 = -4.84141m^{0.5}$$
$$A_2 = 36.88545m^{0.5} + 1.66599m - 0.68730m^{1.5} + 0.12070m^2$$
$$B_2 = -1669.55918\,m^{0.5}$$
$$C_2 = -5.83555m^{0.5}$$

H_2S solubility and dissociation parameters: The interaction parameters involved in H_2S solubility calculation can be estimated from the following generalized equation as a function of pressure and temperature:

$$\begin{aligned}\mathrm{Par}(T,P) &= C_1 + C_2T + C_3/T + C_4\times T^2 + C_5/(630-T) + C_6P \\ &+ C_7P/(680-T) + C_8P^2/T\end{aligned} \quad (36)$$

The constants (C_1-C_8) in the above equation for the H_2S solubility is different from constants in Eq. (32) and it is provided in Table 7.

The procedure requires estimating first and second dissociation constants (K_1 and K_2) of hydrogen sulfide using a correlation (Hershey *et al*., 1988), which is valid for temperature up to 572°F and salt concentration of 6 M. The pK_1 of H_2S (i.e., pK_1 = -log (k_1)) in pure water can be estimated as:

$$pK_{H_2S,1} = 32.55 + 1519.44/T - 15.67\log T + 0.027T \quad (37)$$

where T is temperature in K. The pKH2S, 1 calculated from Eq. (37) needs to be corrected for salinity effect. Thus:

$$\begin{aligned}pK^*_{H_2S,1} &= pK_{H_2S,1} - 0.78708I^{0.5} \\ &+ 0.50475I - 0.05134713I^{1.5}\end{aligned} \quad (38)$$

where, I is the molar concentration of the salt.

CH_4 Solubility Parameters: The interaction parameters involved in CH_4 solubility calculation can be estimated from the following generalized equation as a function of pressure and temperature:

$$\begin{aligned}\mathrm{Par}(T,P) &= C_1 + C_2T + C_3/T + C_4.T^2 + C_5/T^2 + C_6P + C_7.PT \\ &+ C_8P/T + C_9P/T^2 + C_{10}.P^2.T\end{aligned} \quad (39)$$

The constants (C_1-C_{10}) in the above equation for the CH_4 solubility are different from constants in Eq. (32) and it is provided in Table 8.

Partial pressure of water vapor: The partial pressure of water vapor in gas phase can be calculated from the following empirical equation:

$$\begin{aligned}\ln\left(\frac{P^S_{H2O}}{P_C}\right) &= \frac{1}{T_r}\left[-7.86(1-T_r)+1.84(1-T_r)^{1.5}-11.79(1-T_r)^3\right] \\ &+ \frac{1}{T_r}\left[22.68(1-T_r)^{3.5}-15.96(1-T_r)^4+1.80(1-T_r)^{7.5}\right]\end{aligned} \quad (40)$$

where, T_r is reducer temperature, T_c and Pc are the critical temperature and pressure of water (T_c = 647.3K and P_c = 220.9 bar), respectively. Fugacity coefficient of water in the gas phase (Eqn.1) can be calculated from the following equation:

$$\varphi_{H_2O} = \exp\left(a_1 + a_2P + a_3P^2 + a_4PT + \frac{a_5P}{T} + \frac{a_6P^2}{T}\right) \quad (41)$$

Parameters in Eq. (41) are presented in Table 9.

REFERENCES

Anderko, A., 2000. Simulation of $FeCO_3$/FeS scale formation using thermodynamic and electrochemical models. Proceeding of the NACE International Conference (CORROSION/00). Orlando, Florida, Paper No. 102.

Anderko, A.M. and R.D. Young, 1999. Simulation of CO_2/H_2S corrosion using thermodynamic and electrochemical models. Proceeding of the NACE International Conference (CORROSION/99). San Antonio, Texas.

Asmara, Y.P. and M.C. Ismail, 2011. Study combinations effects of HAc in H_2S/CO_2 corrosion. J. Appl. Sci., 11(10): 1821-1826.

Bich, N.N. and K. Goerz, 1996. Caroline pipeline failure: Findings on corrosion mechanisms in wet sour gas systems containing significant CO_2. Proceeding of the NACE International Conference (CORROSION/96). Denver, Colorado.

Brown, B., S. Nesic and S.R. Parakala, 2004. CO_2 corrosion in the presence of trace amounts of H_2S. Proceeding of the NACE International Conference (CORROSION/04). New Orleans, Louisiana, Paper No. 736.

Choi, Y.S. and S. Nešić, 2011. Determining the corrosive potential of CO_2 transport pipeline in high P_{CO2}–water environments. Int. J. Greenh. Gas Con., 5(4): 788-797.

Duan, Z. and R. Sun, 2003. An improved model calculating CO_2 solubility in pure water and aqueous NaCl solutions from 273 to 533 K and from 0 to 2000 bar. Chem. Geol., 193(3-4): 257-271.

Duan, Z. and S. Mao, 2006. A thermodynamic model for calculating methane solubility, density and gas phase composition of methane-bearing aqueous fluids from 273 to 523 K and from 1 to 2000 bar. Geochim. Cosmochim. Ac., 70(13): 3369-3386.

Duan, Z., R. Sun, R. Liu and C. Zhu, 2007. Accurate thermodynamic model for the calculation of H_2S solubility in pure water and brines. Energ. Fuels, 21(4): 2056-2065.

Fang, H., B. Brown and S. Nešić, 2010. High salt concentration effects on CO_2 corrosion and H_2S corrosion. Proceeding of the NACE International Conference (CORROSION/10). San Antonio, Texas, Paper No. 10276.

Fardisi, S., N. Tajallipour and P.J. Teevens, 2012. Predicting general corrosion rates in sour environments with the growth of a protective iron sulphide film. Proceeding of the NACE International Conference (CORROSION/12). Salt Lake City, Utah, Paper No. 1471.

Hershey, J.P., T. Plese and F.J. Millero, 1988. The pK_1* for the dissociation of H_2S in various ionic media. Geochim. Cosmochim. Ac., 52(8): 2047-2051.

Ikeda, A., M. Ueda and S. Mukai, 1985. Influence of environmental factors on corrosion in CO_2 source well. Proceeding of the Technical Symposia on Advances in CO_2 Corrosion. NACE, Houston, TX, 2: 1-22.

Jingen, D., Y. Wei, L., Xiaorong and D. Xiaoqin, 2011. Influence of H_2S content on CO_2 corrosion behaviors of N80 tubing steel. Pet. Sci. Technol., 29(13): 1387-1396.

Kumar, A., J.L. Pacheco, S.K. Desai, W. Huang, R.V. Reddy, W. Sun and C.A. Haarseth, 2014. Selecting representative laboratory test conditions for mildly sour Sulfide Stress Corrosion (SSC) testing. Proceeding of the NACE International Conference (CORROSION/14). San Antonio, Texas, Paper No. 4243.

Kvarekval, J., R. Nyborg and H. Choi, 2003. Formation of multilayer iron sulfide films during high temperature CO_2/H_2S corrosion of carbon steel. Proceeding of the NACE International Conference (CORROSION/03). San Diego, California, Paper No. 339.

Kvarekval, J., A. Dugstad, I.H. Omar and Y.M. Gunaltun, 2005. H_2S corrosion of carbon steel under simulated kashagan field conditions. Proceeding of the NACE International Conference (CORROSION/05). Houston, Texas, Paper No. 300.

Li, C., S. Desai, J. Pacheco, F. Cao and S. Ling, 2013. Effect of sodium chloride concentration on carbon steel sour corrosion. Proceeding of the NACE International Conference (CORROSION/13). Orlando, Florida, Paper No. 2486.

Li, C., Y. Xiong, J.L. Pacheco, F. Cao, S.K. Desai and S. Ling, 2014. Effect of wall shear stress on sour corrosion of carbon steel. Proceeding of the NACE International Conference (CORROSION/14). San Antonio, Texas, Paper No. 4051.

Li, W.F., Y.J. Zhou and Y. Xue, 2012. Corrosion behavior of 110S tube steel in environments of high H_2S and CO_2 content. J. Iron Steel Res. Int., 19(12): 59-65.

Mao, S. and Z. Duan, 2006. A thermodynamic model for calculating nitrogen solubility, gas phase composition and density of the N_2–H_2O–NaCl system. Fluid Phase Equilibr., 248(2): 103-114.

Meyssami, B., M.O. Balaban and A.A. Teixeira, 1992. Prediction of pH in model systems pressurized with carbon dioxide. Biotechnol. Prog., 8(2): 149-154.

Millero, F.J., 1986. The thermodynamics and kinetics of the hydrogen sulfide system in natural waters. Mar. Chem., 18(2-4): 121-147.

Millero, F., F. Huang, T. Graham and D. Pierrot, 2007. The dissociation of carbonic acid in NaCl solutions as a function of concentration and temperature. Geochim. Cosmochim. Ac., 71(1): 46-55.

Mohamed, M.F., A. Mohamed Nor, M.F. Suhor, M. Singer, Y.S. Choi and S. Nesic, 2011. Water chemistry for corrosion prediction in high pressure CO_2 environments. Proceeding of the NACE International Conference (CORROSION/11). Houston, Texas, Paper No. 11375.

Mohammed Nor, A., M.F. Suhor, A.Z. Abas and S. Mat, 2014. Effect of CO_2/H_2S on corrosion behavior of API 5L 65 carbon steel in high P_{CO2} environments. Proceeding of the Offshore Technology Conference-Asia, 2014. Kuala Lumpur, Malaysia, Paper No. OTC-24962-MS.

Nešic, S. and K.L.J. Lee, 2003. A mechanistic model for CO_2 corrosion of mild steel in the presence of protective iron carbonate films - part Ш: Film growth model. Corrosion, 59: 616.

Nešić, S., H. Li, J. Huang and D. Sormaz, 2009. An open source mechanistic model for CO_2 / H_2S corrosion of carbon steel. Proceeding of the NACE International Conference (CORROSION/09). Atlanta, Georgia, Paper No. 572.

Nešić, S., M. Nordsveen, R. Nyborg and A. Stangeland, 2003. A mechanistic model for carbon dioxide corrosion of mild steel in the presence of protective iron carbonate films-Part 2: A numerical experiment. Corrosion, 59(6): 489-497.

Nesic, S., S. Wang, H. Fang, W. Sun and J.K.L. Lee, 2008. A new updated model of CO_2/H_2S corrosion in multiphase flow. Proceeding of the NACE International Conference (CORROSION/08). New Orleans, Louisiana, Paper No. 535.

Nordsveen, M., S. Nešić, R. Nyborg and A. Stangeland 2003. A mechanistic model for carbon dioxide corrosion of mild steel in the presence of protective iron carbonate films—Part 1: Theory and verification. Corrosion, 59(5): 443-456.

Rumpf, B., H. Nicolaisen, C. Öcal and G. Maurer, 1994. Solubility of carbon dioxide in aqueous solutions of sodium chloride: Experimental results and correlation. J. Solution Chem., 23(3): 431-448.

Schmitt, G., 1991. Effect of elemental sulfur on corrosion in sour gas systems. Corrosion, 47(4): 285-308.

Schutt, H.U. and F.F. Lyle, 1998. CO_2/H_2S Corrosion under wet gas pipeline conditions in the presence if bicarbonate, chloride, and oxygen. Proceeding of the NACE International Conference (Corrosion/98). San Diego, California.

Singer, M., S. Nesic, B.N. Brown and A.C. Manuitt, 2007. Combined effect of CO_2, H_2S and acetic acid on bottom of the line corrosion. Proceeding of the NACE International Conference (CORROSION/07). Nashville, Tennessee.

Singer, M., A. Camacho, B. Brown and S. Nesic, 2010. Sour top of the line corrosion in the presence of acetic acid. Proceeding of the NACE International Conference (CORROSION/10). San Antonio, Texas, Paper No. 10100.

Smith, S.N. and J.L. Pacheco, 2002. Prediction of corrosion in slightly sour environments. Proceeding of the NACE International Conference (CORROSION/02). Denver, Colorado.

Srinivasan, S. and R.D. Kane, 1996. Prediction of corrosivity of CO_2/H_2S production environments. Proceeding of the NACE International Conference (CORROSION/96). Denver, Colorado.

Sun, W. and S. Nesic, 2007. A mechanistic model of H_2S corrosion of mild steel. Proceeding of the NACE International Conference (CORROSION/07). Nashville, Tennessee, Paper No. 07655.

Sun, W. and S. Nešić, 2009. A mechanistic model of uniform hydrogen sulfide/carbon dioxide corrosion of mild steel. Corrosion, 65(5): 291-307.

Sun, W., S. Nesic and S. Papavinasam, 2006. Kinetics of iron sulfide and mixed iron sulfide/carbonate scale precipitation in CO_2/H_2S corrosion. Proceedingsof the NACE International Conference (Corrosion/06). San Diego, California, Paper No. 6644.

Sun, W., S. Nešić, D. Young and R.C. Woollam, 2008. Equilibrium expressions related to the solubility of the sour corrosion product mackinawite. Ind. Eng. Chem. Res., 47(5): 1738-1742.

Svenningsen, G., A. Palencsár and J. Kvarekvå, 2009. Investigation of iron sulfide surface layer growth in aqueous H_2S/CO_2 environments. Proceeding of the NACE International Conference (CORROSION/09). Atlanta, Georgia.

Takenouchi, S. and G.C. Kennedy, 1965. The solubility of carbon dioxide in NaCl solutions at high temperatures and pressures. Am. J. Sci., 263(5): 445-454.

Valdes, A., R. Case, M. Ramirez and A. Ruiz, 1998. The effect of small amounts of H_2S on CO_2 corrosion of a carbon steel. Proceeding of the NACE International Conference (CORROSION/98). San Diego, California, Paper No. 22.

Videm, K. and J. Kvarekvål, 1995. Corrosion of carbon steel in carbon dioxide-saturated solutions containing small amounts of hydrogen sulfide. Corrosion, 51(4): 260-269.

Woollam, R., K. Tummala, J. Vera and S. Hernandez, 2011. Thermodynamic prediction of $FeCO_3$/FeS corrosion product films. Proceeding of the NACE International Conference (CORROSION/11). Houston, Texas.

Yan, W., J. Deng, P. Zhu and X. Xing, 2015. Investigation of P_{H2S} influence on 3% Cr tubing steel corrosion behaviours in CO_2-H_2S-Cl^- environment. Corros. Eng. Sci. Techn., 50(7): 525-532.

Yin, Z.F., W.Z. Zhao, Z.Q. Bai, Y.R. Feng and W.J. Zhou, 2008. Corrosion behavior of SM 80SS tube steel in stimulant solution containing H_2S and CO_2. Electrochim. Acta, 53(10): 3690-3700.

Zhang, L., R.M. Ding, J.W. Yang and M.X. Lu, 2009. Analysis of corrosion scales on X60 steel under high H_2S/CO_2 content environments. J. Univ., Sci. Technol. Beijing, 31(5): 563-567.

Zhang, L., W. Zhong, J. Yang, T. Gu, X. Xiao and M. Lu, 2011. Effects of temperature and partial pressure on H_2S/CO_2 corrosion of pipeline steel in sour conditions. Proceeding of the NACE International Conference (CORROSION/11). Houston, Texas.

Zheng, Y., J. Ning, B. Brown and S. Nesic, 2014. Electrochemical model of mild steel corrosion in a mixed H_2S/CO_2 aqueous environment. Proceeding of the NACE International Conference (CORROSION/14), Paper No. 3907.

Zirrahi, M., R. Azin, H. Hassanzadeh and M. Moshfeghian, 2012. Mutual solubility of CH_4, CO_2, H_2S, and their mixtures in brine under subsurface disposal conditions. Fluid Phase Equilibr., 324: 80-93.